Applied Surface Science 256 (2009) 998–1002

Contents lists available at ScienceDirect

Applied Surface Science

journal homepage: www.elsevier.com/locate/apsusc

Zinc oxide nanostructures for applications as ethanol sensors and dye-sensitized solar cells

Supab Choopun *, Auttasit Tubtimtae, Theerapong Santhaveesuk, Sanpet Nilphai, Ekasiddh Wongrat, Niyom Hongsith

Department of Physics and Materials Science, Faculty of Science, Chiang Mai University, Chiang Mai 50200 and ThEP center, CHE, Bangkok 10400, Thailand

ARTICLE INFO

Article history:
Available online 6 June 2009

PACS:
81.05.Dz
81.10.Bk
81.65.Mq
73.61.GA
82.47.Jk

Keywords:
Zinc oxide
ZnO
Nanostructure
Sensor
Dye-sensitized solar cell
Solar cell

ABSTRACT

ZnO nanostructures were prepared by thermal oxidation technique for applying as ethanol sensors and dye-sensitized solar cells. To improve sensitivity of the sensor based on ZnO nanostructures, gold doping was performed in ZnO nanostructures. Gold-doped with 0%, 5%, and 10% by weight were investigated. The improvement of sensor sensitivity toward ethanol due to gold doping was observed at entire operating temperature and ethanol concentration. The sensitivity up to 145 was obtained for 10% Au-doped ZnO sensor. This can be explained by an increase of the quantity of oxygen ion due to catalytic effect of gold. Also, it was found that oxygen ion species at the surface of the Au-doped ZnO sensor remained O^{2-} as pure ZnO sensor. For dye-sensitized solar cell application, the dye-sensitized solar cell structure based on ZnO as a photoelectrode was FTO/ZnO/Eosin-Y/electrolyte/Pt counter electrode. ZnO with different morphologies of nanobelt, nano-tetrapod, and powder were investigated. It was found that DSSCs with ZnO powder showed higher photocurrent, photovoltage and overall energy conversion efficiencies than that of ZnO nanobelt and ZnO nano-tetrapod. The best results of DSSCs were the short circuit current (J_{sc}) of 1.25 mA/cm^2, the open circuit voltage (V_{oc}) of 0.45 V, the fill factor (FF) of 0.65 and the overall energy conversion efficiency (η) of 0.68%.

1. Introduction

ZnO is one of a promising semiconductor material for applications as ethanol sensors and dye sensitized solar cells (DSSCs) [1]. Many researchers have attempted to improve the performance of these devices. For ethanol sensor applications, metal doping is a typical method used to improve sensing properties. The metals such as Au, Pt, and Pd act as catalyst to modify surface reactions of semiconducting metal oxides toward sensing gases. Several works have been reported on the enhancement of sensitivity and stability of sensors that were doped with metal catalyst [2,3]. Moreover, ZnO has nearly the same band gap (3.3 eV) and electron affinity as TiO_2, making it a good candidate as an effective DSSC semiconducting photoelectrode [4]. Additionally, there is a lot of information regarding the processing and a large variety of morphologies of ZnO that can be easily prepared by vapor deposition, solution growth methods, pulsed laser ablation, sputtering, and thermal evaporation [5–10]. The various morphologies of ZnO should be a crucial parameter on the performance of DSSC. In this work, we report on ethanol sensors based on gold-doped ZnO nanostructures and DSSCs based on ZnO with different morphologies as a photoelectrode.

2. Experimental

2.1. Ethanol sensor

Gold-doped zinc oxide nanostructures were prepared by thermal oxidation technique. Mixture of zinc powder and gold powder of 0%, 5%, and 10% by weight were screened as a thick film onto alumina substrate using polyvinyl alcohol for a binder and then, sintered at 700 °C under oxygen atmosphere with flow rate of 500 ml/min for 24 h. The ZnO nanostructures were characterized using field emission scanning electron microscopy (FE-SEM) for morphology. These gold-doped ZnO nanostructures were used to fabricate ethanol sensors by contacting gold interdigital electrodes on the top of surface and putting nickel–chromium coil heater underneath the alumina substrate. The ethanol sensing properties were studied by measuring resistance change in air and in ethanol ambient with ethanol concentration of 50–1000 ppm and at operating temperatures of 300–380 °C. For further application as

* Corresponding author. Tel.: +66 53 943375; fax: +66 53 357511.
E-mail addresses: supab@science.cmu.ac.th, supab99@gmail.com (S. Choopun).

0169-4332/$ – see front matter © 2009 Elsevier B.V. All rights reserved.
doi:10.1016/j.apsusc.2009.05.139

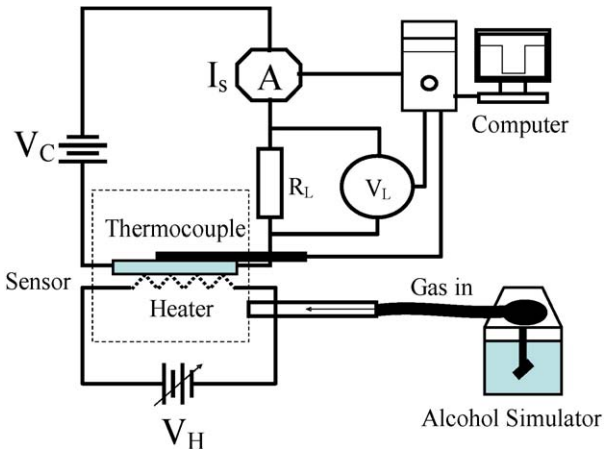

Fig. 1. Schematic circuit diagram used in the sensor characterization experiments.

alcohol breath analyzer, the ethanol vapor at various concentrations was generated from ethanol solutions using alcohol simulator. The sensitivity is defined as the ratio of the electrical resistance of sensor in air (R_a) and in ethanol–air mixed gas (R_g). The operating temperature was measured by a thermocouple placed in the middle of the gas sensor which interfaced to data acquisition. The schematic circuit diagram used in the sensor characterization experiments was shown in Fig. 1.

2.2. Dye-sensitized solar cell

The DSSC structure based on ZnO as a photoelectrode was FTO/ZnO/Eosin-Y/electrolyte/Pt counter electrode. ZnO with different morphologies were prepared on FTO (fluorine-doped SnO_2) glasses by screening technique. The thick films of ZnO nanobelt, nano-tetrapod and powder were fabricated by mixed them with polyethylene glycol solution with ZnO contents of 50% by weight and coated on conducting glass (fluorine-doped SnO_2 glass with a sheet resistance of 8 Ω/square). ZnO nanobelts and nano-tetrapods were prepared by the thermal oxidation reaction technique. The thermal oxidation was performed by heating zinc paste prepared from zinc powder (purity 99.9%) mixed with hydrogen peroxide solution (30 wt.%) at a temperature of 1000 °C under normal atmosphere for a few minutes.

The ZnO thick films were then allowed to dry in air. After air drying, the electrode was sintered for 1 h at 400 °C in air. Adsorption of the dye on the ZnO surface was performed by

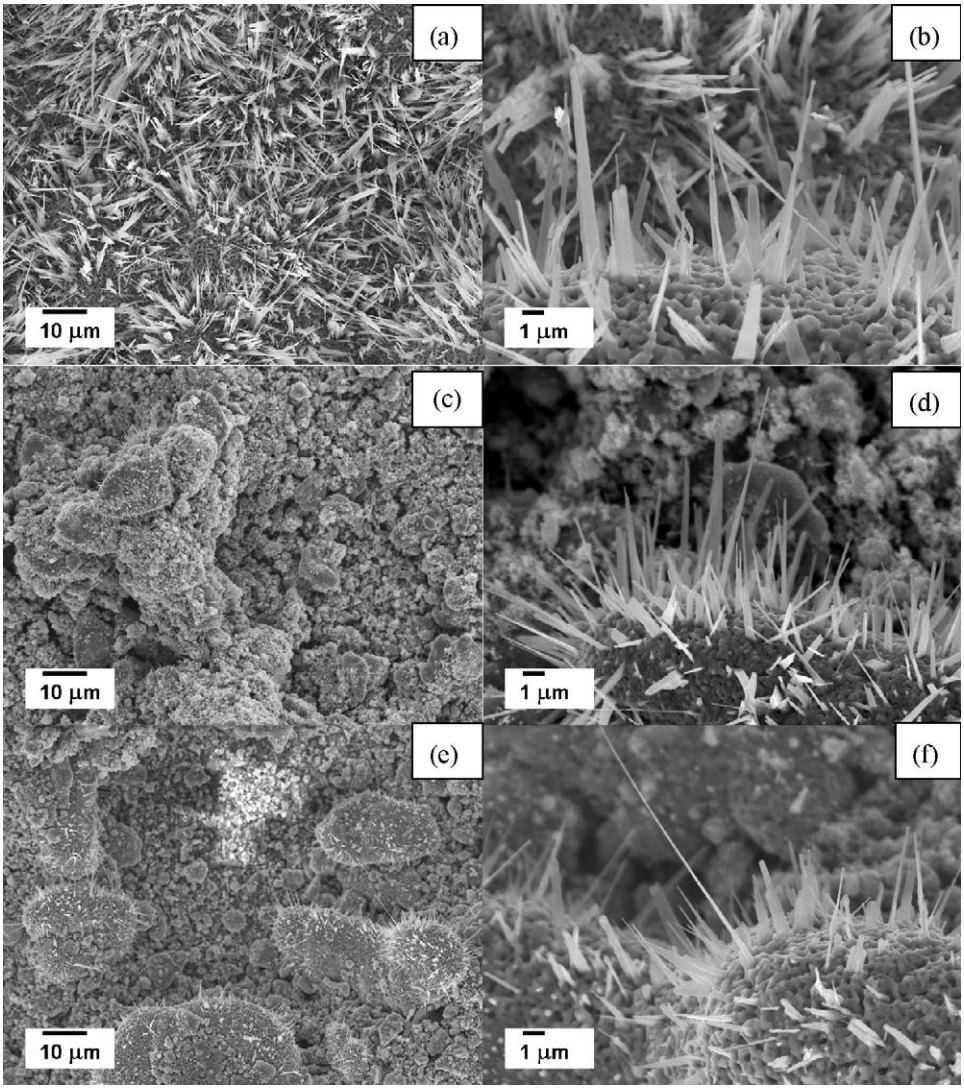

Fig. 2. FE-SEM images of ZnO nanostructure: (a) and (b) for 0% of Au-doped (pure ZnO), (c) and (d) for 5% of Au-doped, (e) and (f) for 10% of Au-doped ZnO nanostructure with magnification of 1000 and 5000, respectively.

refluxing the ZnO electrode in 0.58 mM dry acetone solution of Eosin-Y ($C_{20}H_6O_5Br_4Na_2$) at 25 °C for 24 h, resulting in a photo-electrode. The apparent surface area of the dye-adsorbed ZnO electrode was 0.5 cm × 2.0 cm. The counter electrode was a thermally platinized conducting glass (5 mM H_2PtCl_6 in acetone solution, sinter at 450 °C on a conducting glass substrate for 1 h). The dye-sensitized ZnO electrode was incorporated into a thin-layer sandwich-type solar cell with a thick parafilm sheet as a spacer. The electrolyte solution, a mixture of 0.03 M I_2 + 0.3 M LiI in an ethylene carbonate, was introduced between the ZnO and counter electrodes. The photocurrent and photovoltage characteristics for DSSCs were measured by solar simulator under illumination of 100 mW/cm^2 (AM-1.5).

3. Results and discussion

3.1. Ethanol sensor

FE-SEM images of nanostructures with 0%, 5%, and 10% Au by weight prepared by thermal oxidation method are shown in Fig. 2(a) and (b) for 0% of Au-doped (pure ZnO), (c) and (d) for 5% of Au-doped, (e) and (f) for 10% of Au-doped with magnification of 1000 and 5000, respectively. The wire-like or belt-like nanostructures with the sharp tips are observed outward from microparticles. The diameter and length of ZnO nanostructures are in the range of 250–880 nm and 1.2–9.6 μm for 0%, 170–540 nm and 1.6–7.4 μm for 5% and 250–790 nm and 0.7–8.3 μm for 10% of Au-doped, respectively. It should be noted that diameter was measured at the middle of nanostructures. Typically, the diameter at the tip of nanostructures is in the order of 10 nm. Moreover, the smallest average diameter of nanostructure was found in the case of 5% Au-doped ZnO nanostructure.

Sensitivities of sensors based on 0%, 5%, and 10% of Au-doped ZnO nanostructures as a function of operating temperature at various ethanol concentrations are plotted in Fig. 3(a)–(c), respectively. Clearly, the sensitivity depended on the operating temperatures and exhibited the highest value at optimum operating temperatures.

Usually, temperature dependence of sensitivity is controlled by two parameters; reaction rate coefficient between adsorbed oxygen ions and ethanol molecules and electron density of sensor. The reaction rate coefficient and electron density exponentially increases as increasing the temperature. However, sensitivity is proportional to reaction rate coefficient but inversely proportional to electron density. These two parameters compete with each other and result in maximum sensitivity at optimum temperature. For 5% and 10% of Au-doped ZnO sensors, the reaction rate coefficient and electron density are different resulting in different optimum temperature.

An increase of sensor sensitivity is observed when doping gold in ZnO nanostructures [11]. The 10% Au-doped ZnO sensor showed the highest sensitivity for all ethanol concentration at operating temperature of 300 °C with value of 30 for 50 ppm, 49 for 100 ppm, 57 for 200 ppm, 109 for 500 ppm and 145 for 1000 ppm, respectively. Moreover, the sensitivity of Au-doped ZnO sensors was higher than pure ZnO sensors at entire operating temperature and ethanol concentration. The improvement of sensitivity due to gold doped of the ZnO nanostructures may have two possible explanations. First, gold causes an increase of the quantity of oxygen ion on the surface due to the catalytic effect of gold [12]. Thus, adsorbed oxygen density increases and results in improvement of sensitivity. Second, the gold particles act as a catalyst for the adsorption reaction between adsorbed oxygen ions and ethanol molecules due to a reduction of activation energy. Thus, reaction rate coefficient increases and results in enhancement of sensitivity.

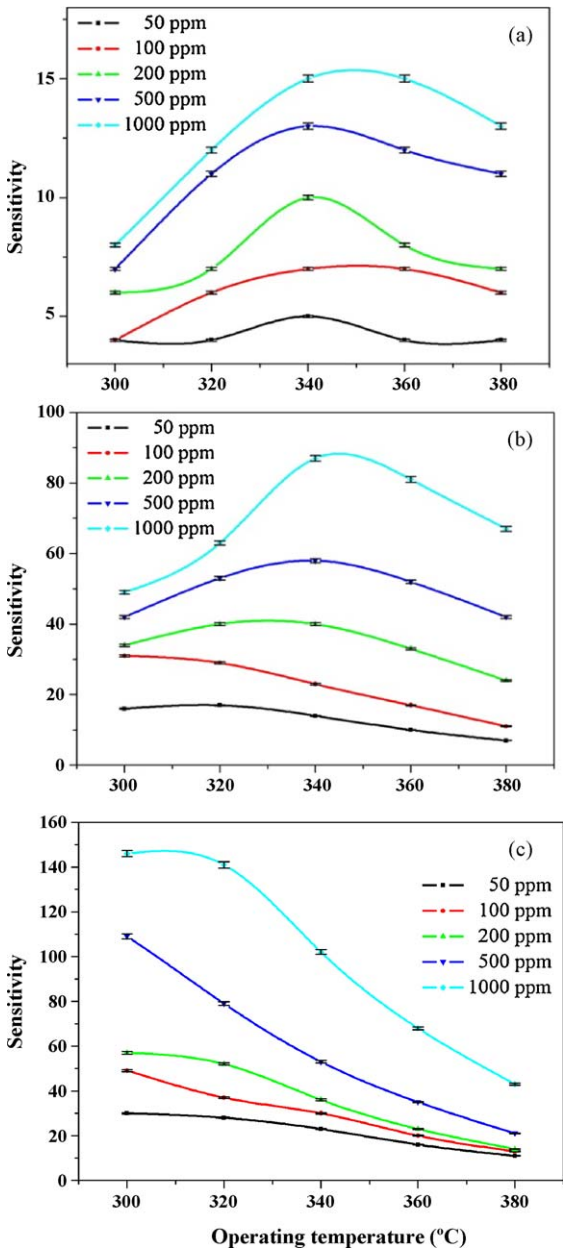

Fig. 3. Plot of sensitivities of sensors based on (a) 0%, (b) 5%, and (c) 10% of Au-doped ZnO nanostructures as a function of operating temperature at various ethanol concentrations.

Usually, gas adsorption on the surface [13–16] can be empirically represented [17,18] as:

$$S = 1 + aC^b \quad (1)$$

where C represents ethanol concentration. The sensitivity S is characterized by the constants a and b. The value of the constant depends on the sensor material and the type of gas sensor which exposed to the operating temperature. The value of the constant b is normally around either 0.5 or 1 that depend on the charge state of the surface ion. It was reported that for b of 0.5 the adsorbed surface oxygen ion is O^{2-} and for b of 1, the adsorbed surface oxygen ion is O^-. Eq. (1) can be rewritten the relation as:

$$\log(S-1) = \log a + b \log C \quad (2)$$

It can be seen that $\log(S-1)$ has linear relation with $\log C$ having a slope of b value. Thus, b value can be obtained from a slope value of a plot between $\log(S-1)$ and $\log C$.

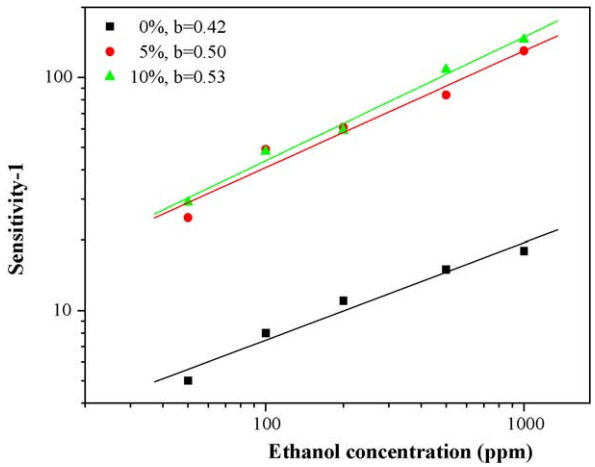

Fig. 4. Plot of $\log(S-1)$ and $\log C$ at the optimum operating temperatures for ethanol sensors based on 0%, 5%, and 10% of Au-doped ZnO nanostructures.

Fig. 4 shows a plot of $\log(S-1)$ and $\log C$ at the optimum operating temperatures for ethanol sensors based on 0%, 5%, and 10% Au-doped ZnO nanostructures. The slope value (b value) is 0.42, 0.50 and 0.53 for 0%, 5%, and 10% Au-doped ZnO nanostructures sensors, respectively. The slope value is nearly 0.5 for all sensors suggesting the adsorbed surface oxygen species on ZnO sensor is O^{2-} [19,20]. It is worth to note that oxygen ion species at the surface does not change from doping with noble metal.

3.2. Dye-sensitized solar cell

Fig. 5 shows FE-SEM images of the ZnO photoelectrode with different morphology. Fig. 5(c) is ZnO powder which has a grain size of about 200–500 nm, (b) shows a nano-tetrapod with leg diameter of about 500 nm, length of about 2–3 μm, and with sharp tips of about 50 nm and (a) shows a nanobelt with thicknesses of about 50–200 nm. The size of the sheets is about 2–5 μm. It can be seen that the size of ZnO powder is less than the nano-tetrapod and nanobelt suggesting the surface-to-volume ratio of ZnO powder is more than that of the nano-tetrapods and nanobelts.

The J–V characteristics of Eosin-Y dye-sensitized solar cells based on ZnO powder, nano-tetrapod and nanobelt are shown in Fig. 6. The energy conversion efficiency (η) and fill factor (FF) derived from the J–V curves are summarized in Table 1. It was found that DSSCs with ZnO powder showed higher photocurrent, photovoltage and overall energy conversion efficiencies than that of ZnO nanobelt and ZnO nano-tetrapod. The best results of DSSCs were the short circuit current (J_{sc}) of 1.25 mA/cm^2, the open circuit voltage (V_{oc}) of 0.45 V, the fill factor (FF) of 0.65 and the overall energy conversion efficiency (η) of 0.68%.

Normally, J_{sc} is directly related to an amount of dye-sensitizer adsorbed on the ZnO surface because the dye sensitizer acts as a photo receiver to absorb a photon, and inject an electron of dye to the conduction band of ZnO to generate current. The highest short circuit current density in ZnO powder DSSC sample is consistent

Table 1
Summary of photoelectrochemical characteristics of DSSCs based on ZnO photoelectrodes with different morphologies.

Morphologies	ZnO powder	ZnO nano-tetrapod	ZnO nanobelt
V_{oc} (V)	0.45	0.43	0.44
J_{sc} (mA/cm^2)	1.25	0.93	0.64
FF	0.65	0.55	0.56
Efficiency (%)	0.68	0.41	0.29

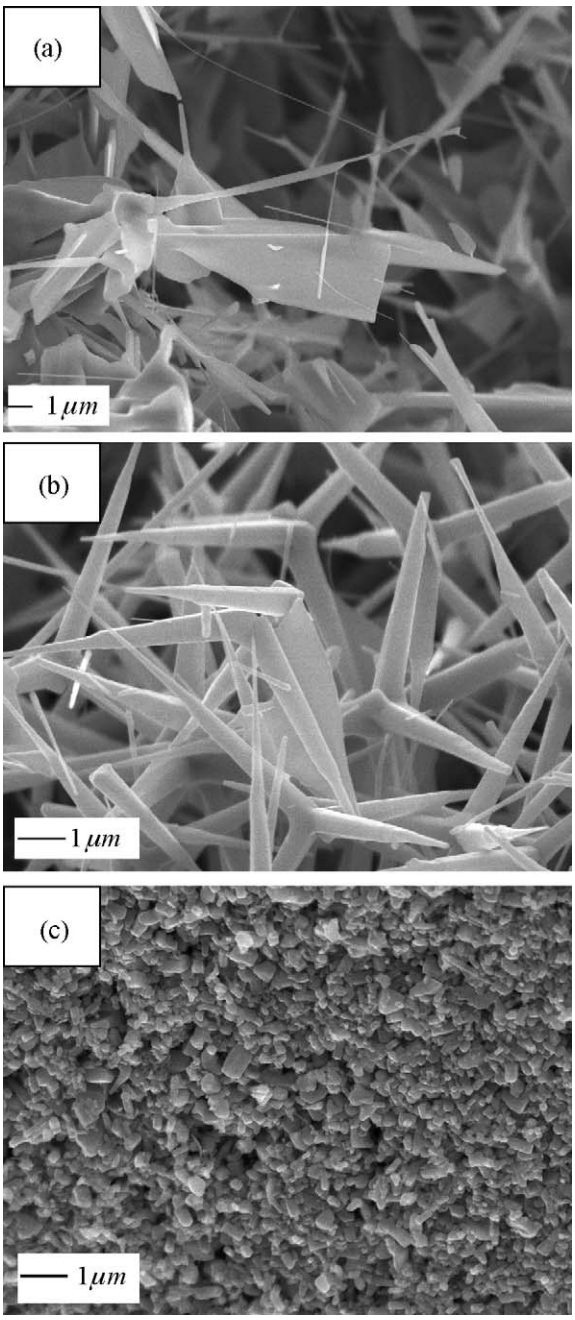

Fig. 5. FE-SEM images of the ZnO photoelectrode with different morphologies (a) nanobelt, (b) nano-tetrapod, and (c) powder.

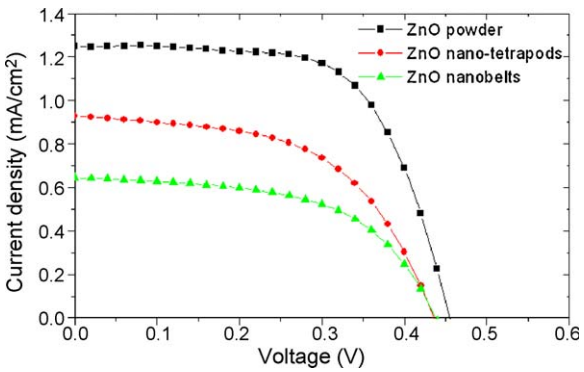

Fig. 6. J–V characteristics of dye-sensitized solar cells based on ZnO powder, nano-tetrapod and nanobelt.

with the FE-SEM results which indicated that ZnO powder has the largest surface-to-volume ratio.

4. Conclusions

ZnO nanostructures were prepared by the thermal oxidation technique for applying as ethanol sensors and dye-sensitized solar cells. Ethanol sensors based on gold-doped ZnO nanostructures with gold of 0%, 5%, and 10% by weight were fabricated and studied the ethanol sensing properties. The improvement of sensor sensitivity toward ethanol due to gold doping was observed at entire operating temperature and ethanol concentration. The sensitivity up to 145 was obtained for 10% Au-doped ZnO sensor. This can be explained by an increase of the quantity of oxygen ion due to catalytic effect of gold. Also, it was found that oxygen ion species at the surface of the Au-doped ZnO sensor remained O^{2-} as pure ZnO sensor. Dye-sensitized solar cells based on ZnO with different morphologies of nanobelt, nano-tetrapod, and powder as a photoelectrode were fabricated and studied photoelectrochemical properties. It was found that DSSCs with ZnO powder showed higher photocurrent (1.25 mA/cm^2), photovoltage (0.45 V) and overall energy conversion efficiency (0.68%) than that of ZnO nanobelt and ZnO nano-tetrapod.

Acknowledgments

This work was supported by Thailand Research Fund (TRF). The financial support from the Graduate School, Chiang Mai University is also acknowledged.

References

[1] D.C. Look, Mater. Sci. Eng. B: Solid State Mater. Adv. Technol. 80 (2001) 383–387.
[2] N. Hongsith, C. Viriyaworasakul, S. Choopun, Ceram. Int. 34 (2008) 823–826.
[3] N.S. Ramgir, Y.K. Hwang, S.H. Jhung, H.-K. Kim, J.-S. Hwang, I.S. Mulla, J.-S. Chang, Appl. Surf. Sci. 252 (2006) 4298–4305.
[4] P. Suri, R.M. Mehra, Sol. Energy Mater. Sol. Cells 91 (6) (2007) 518–524.
[5] M.J. Zheng, L.D. Zhang, G.H. Li, W.Z. Shen, Chem. Phys. Lett. 363 (2002) 123–128.
[6] B.D. Yao, Y.F. Chan, N. Wang, Appl. Phys. Lett. 81 (2002) 757–759.
[7] W.I. Park, D.H. Kim, S.-W. Jung, G.-C. Yi, Appl. Phys. Lett. 80 (2002) 4232–4234.
[8] S. Choopun, H. Tabata, T. Kawai, J. Cryst. Growth 274 (2005) 167–172.
[9] S. Choopun, N. Hongsith, S. Tanunchai, T. Chairuangsri, C. Kruain, S. Singkarat, T. Vilaithong, P. Mangkorntong, N. Mangkorntong, J. Cryst. Growth 282 (2005) 365–369.
[10] S. Choopun, N. Hongsith, E. Wongrat, T. Kamwanna, S. Singkarat, P. Mangkorntong, N. Mangkorntong, J. Am. Ceram. Soc. 91 (2008) 174–177.
[11] A. Tubtimtae, S. Choopun, A. Gardchareon, P. Mangkorntong, N. Mangkorntong, in: Proceedings of the 2nd Annual IEEE Int. Conf. on Nano/Micro Engineered and Molecular Systems, Bangkok, Thailand, (2007), pp. 207–210.
[12] C. Li, L. Li, Z. Du, H. Yu, Y. Xiang, Y. Li, Y. Cai, T. Wang, Nanotechnology 19 (2008) 035501.
[13] Q. Wan, Q.H. Li, Y.J. Chen, T.H. Wang, X.L. He, J.P. Li, C.L. Lin, Appl. Phys. Lett. 84 (2004) 3654–3656.
[14] Z.L. Wang, J. Phys.: Condens. Matter 16 (2004) R829–R858.
[15] T. Gao, T.H. Wang, Appl. Phys. Lett. A80 (2005) 1451–1454.
[16] Y. Ma, W.L. Wang, K.L. Liao, Y. Kong, J. Wide Bandgap Mater. 10 (2002) 113–120.
[17] S.C. Naisbitt, K.F.E. Pratt, D.E. Williams, I.P. Parkin, Sens. Actuators B: Chem. 114 (2006) 969–977.
[18] D.E. Williams, Sens. Actuators B: Chem. 57 (1999) 1–16.
[19] S. Choopun, N. Hongsith, P. Mangkorntong, N. Mangkorntong, Zinc oxide nanobelts by RF sputtering for ethanol sensor, Physica E 39 (2007) 53–56.
[20] E. wongrat, P. Pimpang, S. Choopun, Appl. Surf. Sci. (2009), doi:10.1016/j.apsusc.2009.02.046.